https://doi.org/10.5194/wes-2022-94
Preprint. Discussion started: 17 October 2022

eawe european academy of wind energy
Open Access WIND ENERGY SCIENCE DISCUSSIONS

A simple vortex model applied to an idealized rotor in sheared inflow

Mac Gaunaa[1], Niels Troldborg[1], and Emmanuel Branlard[2]
[1]DTU Wind & Energy Systems, Frederiksborgvej 399, 4000, Roskilde, Denmark
[2]National Renewable Energy Laboratory, 15013 Denver West Parkway, Golden, CO 80401, USA
Correspondence: Mac Gaunaa (macg@dtu.dk)

Abstract. A simple analytical vortex model is presented and used to study an idealized wind turbine rotor in uniform and sheared inflow, respectively. The work reveals that locally 1D momentum theory is valid for a non-uniformly loaded rotor in a sheared inflow. Hence the maximum local power coefficient (expressed with respect to the local, upstream velocity) of an ideal rotor is not affected by the presence of shear. We study the interaction between the wake vorticity generated by the rotor and the wind shear vorticity, and find that their mutual interaction results in no net generation of axial vorticity: the wake effects and the shear effects exactly cancel each other out. This means that there is no resulting cross-shear induced velocities and therefore also no cross-shear deflection of the wake in this model.

1 Introduction

The atmospheric shear layer significantly affects the power production and loads of wind turbines, and it is therefore essential to accurately model wind turbines under sheared inflow. However, recent validation studiesBoorsma et al. (2022) have shown that state-of-the-art models show some significant deficiencies in modeling wind turbine performances under wind shear conditions. Madsen et al. (2012) simulated a wind turbine operating under strong shear condition using different Blade Element Momentum (BEM) based models and compared the results to the ones obtained with more advanced tools. The authors concluded that for the simulation of wind turbines under sheared inflow, BEM-based formulations need to be expressed using local relations, that is, the local induction factor needs to be defined using the local free-stream velocity. Furthermore, they compared the power obtained in sheared and non-sheared inflows for identical velocities at hub-height. The authors found that, in most cases, a lower power production was obtained in sheared inflow compared to cases without shear, in spite of the total available power in the incoming wind being higher for the shear case. They explained this with the fact that, over most of a revolution period, the turbine blades operate away from their optimal conditions when the inflow is nonuniform.

Shen et al. (2011) and Sezer-Uzol and Uzol (2013) used free vortex wake vortex models to simulate horizontal axis wind turbine in sheared inflow and also found that the power output in that case is lower than in uniform inflow.

However, the computational fluid dynamics simulations conducted by Zahle and Sørensen (2010), which were also included in the work by Madsen et al. (2012), indicated that the power production was increased when operating in shear with a proportion that can be largely explained by the increase in available power in the upstream flow. By analysing the local power coefficient (expressed with respect to the local, upstream velocity) they observed higher efficiencies on the lower half of the rotor which was explained by differences in local angle of attack and tip speed ratio between the lower and upper half of the rotor. A similar

https://doi.org/10.5194/wes-2022-94
Preprint. Discussion started: 17 October 2022

eawe european academy of wind energy
Open Access WIND ENERGY SCIENCE DISCUSSIONS

effect was found in the analytical model by Magnusson (1999) although he did not investigate the effect of shear on the total power of the turbine. The simulations by Zahle and Sørensen (2010) furthermore showed that the flow field upstream of the rotor had a a significant downward velocity component, causing high velocity air from higher altitudes to flow through the lower half of the rotor. It was argued that this phenomenon also could play a role in the increased power production at the lower part of the rotor disc. Another effect observed from their simulations is the asymmetric development of the wake due to the interaction of wake rotation and shear, which in effect led to a different loading on the blade when pointing to the left than when pointing to the right.

Chamorro and A Arndt (2013) derived a simple analytical correction for the maximum efficiency of an ideal wind turbine rotor in non-uniform inflow which accounts for the non-uniform velocity through the so-called Boussinesq and Coriolis correction factors. Their study revealed that the maximum power of a turbine in a typical neutrally stratified boundary layer may increase by between 1-2%. However, a closer inspection of their work reveals that the predicted power increase in fact is exactly equal to the increase in available power in the inflow. Therefore, they essentially show that the maximum power coefficient based on the available power in the incoming wind is unchanged for rotors in shear.

Micallef et al. (2010) modeled a wind turbine wake in sheared inflow using oblique vortex rings and obtained an analytical solution for the wake deflection. The ring inclination induces a vertical velocity component and the model therefore predicts an upward deflection of the wake. This result agrees with predictions obtained using various free vortex vortex tools (Sezer-Uzol and Uzol (2013); Grasso (2010).) Branlard et al. (2015) showed that the nonphysical upward deflection of the wake observed in earlier studies using vortex methods is caused by neglecting the vorticity imposed by the inflow shear. They proposed both a frozen and unfrozen inflow shear model to avoid the upward deflection. In both approaches the velocity and vorticity is split into a prescribed part due to inflow shear and a varying part due to e.g inflow turbulence or wakes. This split of scales is similar to that proposed by Troldborg et al. (2014) in their simplified CFD based model of the atmospheric boundary layer. In the frozen approach it is then assumed that the additional vorticity imposed by the varying part does not affect the prescribed field, whereas a full interaction is allowed in the unfrozen approach. They implemented the two methods in a vortex particle solver and used them together with an actuator disk model to simulate the wake of turbine in sheared and turbulent inflow. They showed that the frozen approach reduced the nonphysical upward wake motion and removed it completely when using the unfrozen approach.

Ramos-García et al. (2018) proposed a prescribed velocity-vorticity atmospheric boundary layer model and implemented it in the vortex solver MIRAS. They used the model together with a lifting line method to simulate the wake of a wind turbine in different sheared and turbulent inflows. Similar to the work of Branlard et al. (2015), they showed that by properly accounting for the shear's contribution to vortex stretching and convection, the upward deflection of the wake was removed. Besides performing thorough investigations of the wake, they also studied the impact of shear and turbulence on the power and loads. They found that the power output of the turbine was augmented slightly with increasing shear.

The above literature review shows that the influence of wind shear on wind turbine rotors is not fully understood and that there is no clear consensus on e.g. its impact on power production. In this paper, we derive an analytical, vortex-based model of an idealized wind turbine rotor to study its operation in sheared inflow and thereby explain some of the main mechanisms at play.

https://doi.org/10.5194/wes-2022-94
Preprint. Discussion started: 17 October 2022

eawe european academy of wind energy
Open Access WIND ENERGY SCIENCE DISCUSSIONS

2 A simple vortex rotor model including shear

The model presented in the following is an extension of work presented by Øye (Madsen et al., 2006; Øye, 1990) and Branlard and Gaunaa (2015). They both modelled an idealized wind turbine with an infinite number of blades located in a uniform steady inflow. However, whereas Øye assumed the blade circulation to be uniform, Branlard and Gaunaa (2015) allowed it to vary radially in their model. In the present treatment, the blade circulation may vary both in the radial and azimuthal direction. The loading at each specific position on the disc is, however, constant in time. For further simplification, we restrict ourselves to the idealized case where the rotational speed tends to infinity. Therefore, wake rotational effects are absent and the situation is similar to the classical 1D momentum results (Betz, 1920; Lanchester, 1915). Two other simplifying assumptions, which open up for a simple analytical treatment of the problem, is to neglect wake expansion and to assume that the convection velocity of the wake vorticity is constant, and determined using the conditions in the far wake. These assumptions were initially proposed by Øye (Øye, 1990), who showed that the results for an uniformly loaded actuator disc in uniform inflow with these assumptions are identical to 1D momentum theory. Finally, we only consider cases where the incoming wind is parallel to the axis of rotation and where the rotor blades are straight and perpendicular to the rotor axis.

2.1 Basic relations

2.1.1 Rotor loads

Our simplified rotor model is derived under the potential-flow assumptions (incompressible, irrotational and inviscid flow), which physically corresponds to low mach-numbers and high Reynolds numbers. We neglect the effects of drag on the rotor performance[1]. The local forces per unit span, at a given radial location of the blade, are therefore obtained using the Kutta-Joukowski relation:

$$\mathbf{f}_b = \rho \mathbf{V}_{\text{rel}} \times \mathbf{\Gamma}_b \tag{1}$$

where $\mathbf{\Gamma}_b$ is the bound circulation distributed and directed along the blade, $\mathbf{V}_{\text{rel}}$ is the relative velocity of a blade element and ρ is the air density. The notations are illustrated in Figure 1. Polar coordinates (r, θ, z) are used, where the unit vector $\hat{\mathbf{z}}$ is normal to the disc and parallel to the main flow, $\hat{\mathbf{r}}$ is along the blade, and the tangential vector , $\hat{\theta}$, is along the direction of rotation. The relative velocity is formed by the local free stream velocity, V_0, which may vary in space, the induced velocity, $\mathbf{W}$, and the relative rotational speed of the element, $-\Omega r$, where Ω is the rotor rotational velocity and r is the radius of the element. The relative velocity is $\mathbf{V}_{\text{rel}} = (V_0 + W_z)\hat{\mathbf{z}} + (-\Omega r + W_\theta)\hat{\theta}$ and the bound circulation associated with one blade is $\mathbf{\Gamma}_b = \Gamma_b \hat{\mathbf{r}}$. The total bound circulation of the rotor at a given radial location of the disc is $\mathbf{\Gamma} = N_b \mathbf{\Gamma}_b$, where N_b is the number of blades.

[1]The effect of profile drag can be added as a post-processing step, see for instance Branlard (2017)

https://doi.org/10.5194/wes-2022-94
Preprint. Discussion started: 17 October 2022

eawe european academy of wind energy
Open Access WIND ENERGY SCIENCE DISCUSSIONS

The local forces per unit area on the rotor disc becomes

$$\mathbf{F} = \begin{bmatrix} F_r \\ F_\theta \\ F_z \end{bmatrix} = \frac{N_b \mathbf{f}_b dr}{2\pi r dr} = \frac{\rho \Gamma \Omega}{2\pi} \begin{bmatrix} 0 \\ (V_0 + W_z)/(\Omega r) \\ 1 - W_\theta/(\Omega r) \end{bmatrix} \tag{2}$$

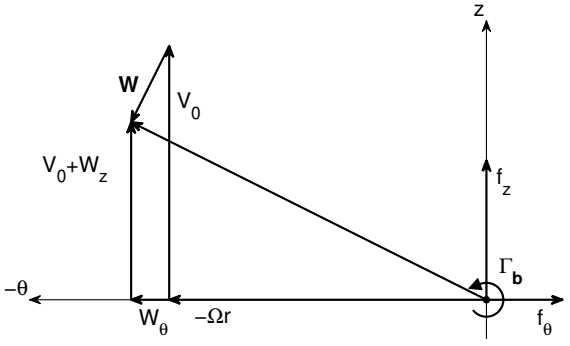

Figure 1. *Cross-section of blade element showing velocity and force vectors.*

where F_r, F_θ and F_z are the polar components of the the local forces per unit area. Introducing the local thrust coefficient, C_t, based on local free stream velocity and local disc load, we obtain the following expression from the axial force component of Equation (2)

$$C_t = \frac{F_z}{0.5\rho V_0^2} = \frac{\Gamma\Omega}{\pi V_0^2}\left(1 - \frac{W_\theta}{\Omega r}\right) \tag{3}$$

Letting Ω go to infinity while retaining a finite value for the product $\Gamma\Omega$ show that Γ tends to zero. This correspond to tangential induced velocities, W_θ, also tending to zero (Branlard and Gaunaa, 2016). Equation (3) therefore reduces to

$$C_t = \frac{\Gamma\Omega}{\pi V_0^2} \tag{4}$$

Since the local power production per area on the rotor is $p = F_\theta \Omega r$ we get

$$p = \frac{dP}{dA} = \frac{\rho\Gamma\Omega}{2\pi}(V_0 + W_z) \tag{5}$$

The local power coefficient is obtained from Equation (5)

$$C_p = \frac{p}{0.5\rho V_0^3} = \frac{\Gamma\Omega}{\pi V_0^2}\left(1 + \frac{W_z}{V_0}\right) \tag{6}$$

In terms of the local axial induction factor $a = -W_z/V_0$, we get by use of Equation (4)

$$C_p = C_t(1 - a), \tag{7}$$

which corresponds exactly to classical 1D momentum theory (Glauert, 1963).

https://doi.org/10.5194/wes-2022-94
Preprint. Discussion started: 17 October 2022

eawe european academy of wind energy
Open Access WIND ENERGY SCIENCE DISCUSSIONS

2.1.2 Wake vorticity

In order to determine the velocity at the rotor disc and in the wake of the disc, the strength of the trailed and shed vortex sheets downstream of the disc is needed. To do this, we will be using the following result, which is proven in Appendix B and illustrated in Figure 2:

For an infinitely long cylinder surface of constant-strength tangential vorticity, $\gamma = d\Gamma/dz$, the induction in the direction of the cylinder axis (z) is γ on the inside and zero on the outside of the cylinder irrespective of its cross-sectional shape. Due to the symmetric properties of vortices, the axial induction at the ending plane of a corresponding half-infinite vortex cylinder is $\gamma/2$.

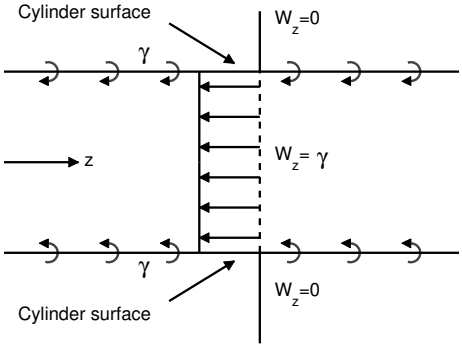

Figure 2. *Sketch of velocity field induced by an infinite cylinder of tangential vortex density γ*

According to Helmholtz first law, all vortex lines must form closed loops, extend to infinity or start/end at solid boundaries. Therefore, any change in bound vorticity in the spanwise direction causes vorticity to be trailed into the wake from the rotor, while variations of the bound vorticity in the tangential direction results in vorticity shed into the wake (see Figures 3 and 4, where a discrete representation of the circulation is used to simplify the discussion). If the bound vorticity on the blade changes from position i to j, the strength of the trailed and/or shed vorticity is given by:

$$\gamma_{i-j} = \frac{\partial \Gamma_b}{\partial z} = \frac{\partial \Gamma_b}{\partial \theta}\frac{\partial \theta}{\partial t}\frac{\partial t}{\partial z} = \frac{\partial \Gamma_b}{\partial \theta}\frac{\Omega}{\dot{z}} = \frac{\Delta\Gamma\Omega}{2\pi\dot{z}} \tag{8}$$

Here $\Delta\Gamma$ denotes the variation in bound vorticity at a given position during one rotor revolution and $\dot{z}$ is the transport velocity of the vorticity sheet in the axial direction. A more thorough derivation of Equation (8) is provided in Appendix A. From Equation (8), it is clear that to determine the strength of the trailed and shed vortex sheets, the convection velocity $\dot{z}$ is needed. This convection velocity is the mean of the velocities on each side of the vortex sheet. In order to simplify the present model, we adopt a generalization of what was shown by Øye (1990) to give good results: a vortex sheet is convected with a constant velocity which is the mean of the velocity on each side of the sheet far downstream of the rotor. Given two regions i and j, the convection velocity is therefore $\dot{z} = (V_{w_i} + v_{w_j})/2$, where V_{w_i} and V_{w_j} are the velocities on each side of the vorticity sheet far downstream of the rotor.

https://doi.org/10.5194/wes-2022-94
Preprint. Discussion started: 17 October 2022

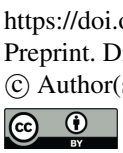

eawe european academy of wind energy
Open Access WIND ENERGY SCIENCE DISCUSSIONS

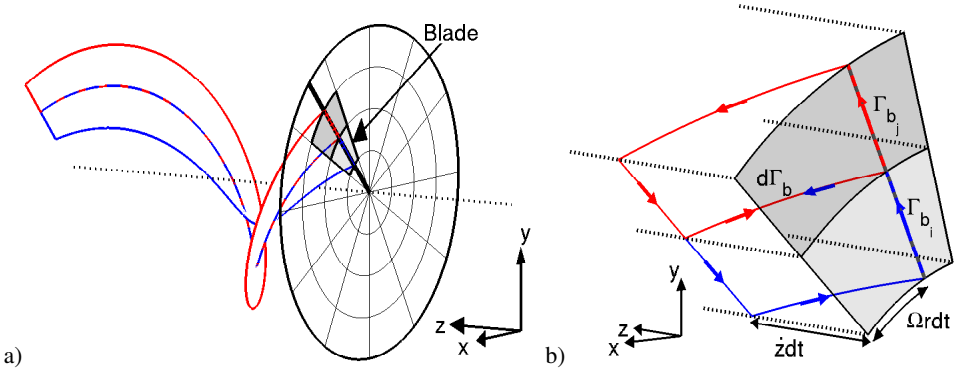

Figure 3. *a) Sketch of vorticity trailed from a blade section, when the bound vorticity changes by $d\Gamma_b = \Gamma_{b_j} - \Gamma_{b_i}$ in the radial direction. b) Close view of the blade section showing the definition of $d\Gamma_b$.*

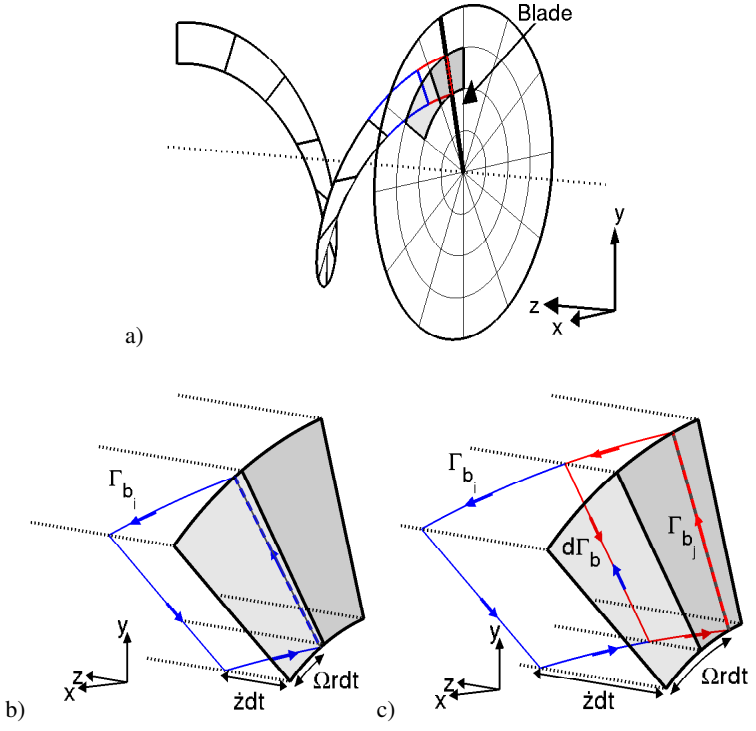

Figure 4. *a) Sketch of vorticity shed from a blade section, when the bound vorticity changes in the tangential direction. b-c) Close view of the blade section at two successive time instances, showing the definition of $d\Gamma_b$.*

Using this assumption together with Equations (4) and (8), the strength of the vorticity sheet released into the wake as a consequence of a local change in loading between two regions i and j on the disc can be expressed as follows:

$$\gamma_{i-j} = \frac{(\Gamma_j - \Gamma_i)\Omega}{2\pi\dot{z}} = \frac{C_{t_j}V_{0_j}^2 - C_{t_i}V_{0_i}^2}{V_{w_j} + V_{w_i}} \tag{9}$$

https://doi.org/10.5194/wes-2022-94
Preprint. Discussion started: 17 October 2022

eawe european academy of wind energy
Open Access WIND ENERGY SCIENCE DISCUSSIONS

where C_{t_i} and C_{t_j} denote the local thrust coefficient of the two regions, respectively, V_{0_i} and V_{0_j} are their corresponding local free-stream velocity.

3 Application of model

3.1 Uniformly loaded rotor in uniform inflow

In this section, we consider a uniformly loaded rotor in uniform inflow. In this case, all the bound vorticity of the disc is trailed from the edge of the disc and thus the vorticity released into the wake is distributed on a cylinder as sketched in Figure 5. The strength of the released vorticity sheet, γ_{0-1}, is determined from Equation (9) and using the assumptions described in

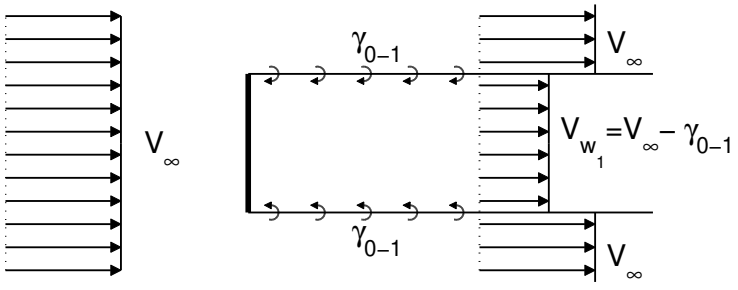

Figure 5. *Schematic view of a uniformly loaded disc in a uniform inflow.*

section 2.1.2:

$$\gamma_{0-1} = \frac{C_{t_1} V_{0_1}^2}{V_{w_1} + V_{w_0}} = \frac{C_T V_\infty^2}{2V_\infty - \gamma_{0-1}} \tag{10}$$

where $C_{t_1} = C_T$ is the thrust coefficient of the disc, $V_{0_1} = V_\infty$ is the free-stream velocity and the subscript $0-1$ indicates that the vorticity is released between the wake (region 1) and the exterior (region 0). Solving for γ_{0-1} yields

$$\gamma_{0-1} = V_\infty(1 - \sqrt{1 - C_T}) \tag{11}$$

The rotor disc is, at the ending plane of a half-infinite vortex cylinder and thus as described in section 2.1.2, the axial velocity here is $V_\infty - \gamma_{0-1}/2 = V_\infty(1-a)$, where a is the axial induction factor. Therefore $\gamma_{0-1} = 2aV_\infty$ and from Equation (11), we get

$$C_T = 4a(1-a) \tag{12}$$

https://doi.org/10.5194/wes-2022-94
Preprint. Discussion started: 17 October 2022

$$V_w = V_\infty - \gamma_{0-1} = V_\infty \sqrt{1 - C_T} = V_\infty (1 - 2a) \tag{13}$$

where V_w is the velocity in the far wake.

Equation (12) and (7) show that the present model and classical 1D momentum theory gives identical results. This is consistent with the conclusion drawn by Øye (1990) and shows that the crude approximations made herein are essentially not worse than the assumptions made in 1D momentum theory.

3.2 Non-uniformly loaded rotor in uniform flow

In this section, we apply the model to a non-uniformly loaded rotor in uniform flow. For simplicity we consider a case where two different load levels are present: C_{t_1} in the lower half of the rotor disc and C_{t_2} in the upper half, see Figure 6. We start by

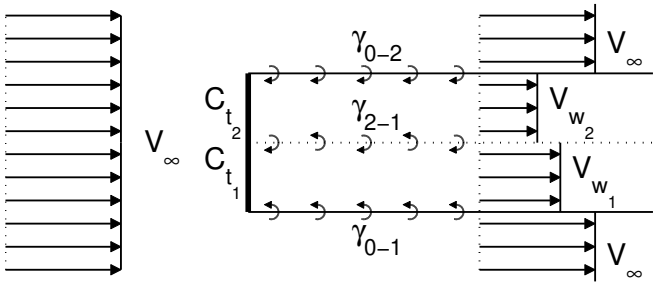

Figure 6. *Schematic view of a non-uniformly loaded disc in a uniform inflow.*

assuming that the axial velocity in the far wake (and therefore also at the rotor disc) is constant in each of the two regions and then later check whether this assumption leads to inconsistencies.

If the axial velocity in each of the far wake regions is constant, its value should be as in the uniformly loaded case, since at the outer edge, the local conditions are as in the uniformly loaded case. Thus, the far wake velocity in each region would be given by Equation (13) and the strength of the sheet released between the two regions would be given by equation (9), i.e.

$$\gamma_{2-1} = \frac{C_{t_1} V_\infty^2 - C_{t_2} V_\infty^2}{V_\infty \sqrt{1 - C_{t_1}} + V_\infty \sqrt{1 - C_{t_2}}} = V_\infty \left(\sqrt{1 - C_{t_2}} - \sqrt{1 - C_{t_1}} \right) \tag{14}$$

In order to have a constant velocity in the wake of each zone this vortex sheet strength should according to the behaviour of vortex cylinders (section 2.1.2) be equal to the difference of the "outer" vortex sheet strengths of each zone. From Equation (11)

https://doi.org/10.5194/wes-2022-94
Preprint. Discussion started: 17 October 2022

eawe european academy of wind energy
Open Access WIND ENERGY SCIENCE DISCUSSIONS

the difference in sheet strengths between the regions from 1 and 2 to the exterior is

$$\gamma_{0-1} - \gamma_{0-2} = V_\infty \left(\sqrt{1 - C_{t_2}} - \sqrt{1 - C_{t_1}} \right) \tag{15}$$

This is exactly equal to Equation (14). If the assumption of a constant velocity in each of the two zones was incorrect, this would not have been the case. The derivation above can readily be extended to a slightly more general case of two regions that both have borders with each other and with the outer flow (and therefore none of the load regions are fully enclosed in the other). In fact, the arguments used in the derivation above also hold in the general case with more than two different load regions including cases where one load region is fully enclosed in other loads regions. Therefore, the present model predicts that any stream element behaves locally as predicted by 1D momentum theory. This is in agreement with the result presented by Johnson (2013) and Branlard and Gaunaa (2015) and consistent with the derivation of the classical axisymmetric blade element theory, where the annular stream tubes are assumed to be independent of each other. However, the present model goes further as it indicates both radial and tangential independence of the individual stream elements. Thus, while one might expect that more air would flow through a lightly loaded part of a non-uniformly loaded rotor in uniform inflow, the present model predicts that this is not the case. Otherwise, the axial velocity (and hence power production, see Equation (6)) on the lighter loaded part of the disc would be higher than what is expected from 1D momentum results.

3.3 Non-uniformly loaded rotor in a step-shear

We now consider a non-uniformly loaded rotor in a planar step-shear inflow, as illustrated in Figure 7. For simplicity, we assume that the rotor has a constant loading of C_{t_1} below the step and another constant loading of C_{t_2} above the step. A step

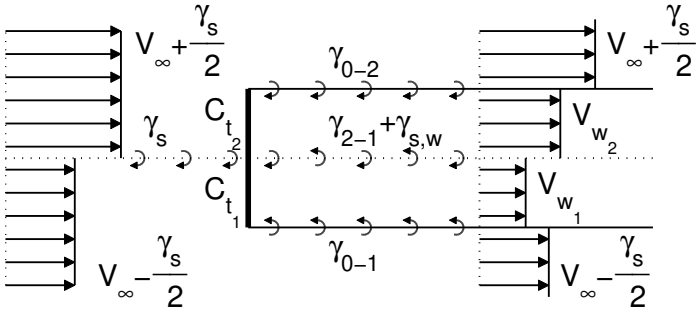

Figure 7. *Schematic view of a non-uniformly loaded disc in a step shear generated by introducing an infinite vorticity sheet of strength γ_s in the horizontal plane through the rotor center.*

shear can be obtained by adding an infinite planar vortex sheet and an uniform flow. If γ_s denotes the shear sheet strength and

https://doi.org/10.5194/wes-2022-94
Preprint. Discussion started: 17 October 2022

eawe european academy of wind energy
Open Access WIND ENERGY SCIENCE DISCUSSIONS

V_∞ denotes the uniform free-stream speed, we get the following far-field, upstream inflow velocities

$$V_0(y, z=-\infty) = \begin{cases} V_{0_1} = V_\infty - \gamma_s/2 & \text{for} \quad y < 0 \\ V_{0_2} = V_\infty + \gamma_s/2 & \text{for} \quad y \geq 0 \end{cases} \tag{16}$$

where y denotes the height above the shear vorticity sheet. The main effect of the rotor is to change the axial velocity of the flow and hence also the convection velocity of the shear sheet in the wake.

Due to steady state conditions, the transport of circulation through any point in the shear-plane is equal to that far upstream:

$$\gamma_s V_\infty = \gamma_{s,w} \dot{z} \tag{17}$$

where $\dot{z} = (V_{w_2} + V_{w_1})/2$ is the mean of the far wake velocities on each side of the shear vorticity layer,and $\gamma_{s,w}$ is the intensity of the shear voticity sheet in the wake. Thus, for a wind turbine the intensity of the shear vorticity sheet is effectively increased in the wake because the axial velocity is lower than in the free stream.

For convenience, the intensity of the shear vorticity sheet in the wake is split as follows:

$$\gamma_{s,w} = \gamma_s + \Delta\gamma_s \tag{18}$$

where γ_s is responsible for the effective backbone velocity (Equation (16)) and $\Delta\gamma_s$ is the additional induced part due to the changed velocity in the wake.

In order to check whether our model is also consistent with 1D momentum theory in the sheared inflow case we proceed as in the previous section and assume that the induced velocities in each region are constant and see whether this leads to any inconsistencies.

If the axial velocity in each of the far wake regions is constant it should be determined from Equation (13), where now the local backbone freestream velocity has to be used:

$$V_{w_i} = V_{0_i}\sqrt{1 - C_{t_i}} = V_{0_i}(1 - 2a_i) \tag{19}$$

where index $i = 1, 2$ refer to the two regions, respectively and where have introduced the local induction factor for region i

$$a_i = \frac{1}{2}\left(1 - \sqrt{1 - C_{t_i}}\right) \tag{20}$$

Inserting equation (19) into equation (9) yields the following expressions for the strength of the vortex sheets released from the rotor:

$$\gamma_{0-1} = \frac{C_{t_1} V_{0_1}}{2 - 2a_1} = V_{0_1}\left(1 - \sqrt{1 - C_{t_1}}\right) \tag{21}$$

$$\gamma_{0-2} = \frac{C_{t_2} V_{0_2}}{2 - 2a_2} = V_{0_2}\left(1 - \sqrt{1 - C_{t_2}}\right) \tag{22}$$

$$\gamma_{2-1} = \frac{C_{t_1} V_{0_1}^2 - C_{t_2} V_{0_2}^2}{V_{0_1}(1 - 2a_1) + V_{0_2}(1 - 2a_2)} \tag{23}$$

https://doi.org/10.5194/wes-2022-94
Preprint. Discussion started: 17 October 2022

Similarly, by inserting equation (19) into equation (17) and using equation (18), we get the following expression for the shear sheet condensation:

$$\Delta\gamma_s = \gamma_s \left(\frac{2V_\infty}{V_{0_2}(1-2a_2) + V_{0_1}(1-2a_1)} - 1 \right) \tag{24}$$

In the far wake, the intensity of the vortex sheet separating the upper and lower part of the wake is

$$\gamma_{2-1,\text{total}} = \gamma_{2-1} + \Delta\gamma_s \tag{25}$$

Inserting Equations (23) and (24) into Equation (25) and rewriting using Equation (19) yields:

$$\gamma_{2-1,\text{total}} = V_{0_2}\sqrt{1-C_{t_2}} - V_{0_1}\sqrt{1-C_{t_1}} - \gamma_s \tag{26}$$

From the basic behaviour of vortex cylinders (section 2.1.2), we know that in order to have a constant induced velocity in the wakes of each of the zones, the total vortex sheet strength between the lower and upper zones is equal to the difference of the "outer" vortex sheet strengths of each zone. From Equations (21) and (22) we get:

$$\begin{aligned} \gamma_{0-1} - \gamma_{0-2} &= V_{0_1}\left(1-\sqrt{1-C_{t_1}}\right) - V_{0_2}\left(1-\sqrt{1-C_{t_2}}\right) \\ &= V_{0_2}\sqrt{1-C_{t_2}} - V_{0_1}\sqrt{1-C_{t_1}} - \gamma_s \end{aligned} \tag{27}$$

As seen, Equation (27) and Equation (26) are identical. Therefore, the initial assumption of a uniform far wake velocity in each region was correct.
The reason why there is no local effect of the shear is that the effect of the changed convection velocity of the wake vorticity ($\dot{z}$), at the shear intersection, is exactly counter weighed by the induced shear vorticity (Equation (24)).

From equations (20) and (7) we get the local thrust and power coefficient:

$$C_{t_i} = 4\, a_i\,(1-a_i) \tag{28}$$

$$C_{p_i} = 4\, a_i\,(1-a_i)^2 \tag{29}$$

which is identical to the classical result from 1D momentum theory. In analogy with the arguments given in the previous section, we conclude that local 1D momentum theory is valid for any load distribution and any 1D shear, under the assumptions made in this work. This is an important result to keep in mind when developing additions to BEM models to make them able to perform sensibly in shear since it shows that such models should be based on local quantities and avoid adopting concepts such as average disc load/induction or average annulus load/induction.

3.4 Formation of cross-shear induced velocities

A basic property of vortex filaments in inviscid flow is that they cannot end in the fluid and therefore both the wake and shear vorticity sheets are deformed under the influence of velocity gradients. This is illustrated in Figure 8, which is a 3D sketch

https://doi.org/10.5194/wes-2022-94
Preprint. Discussion started: 17 October 2022

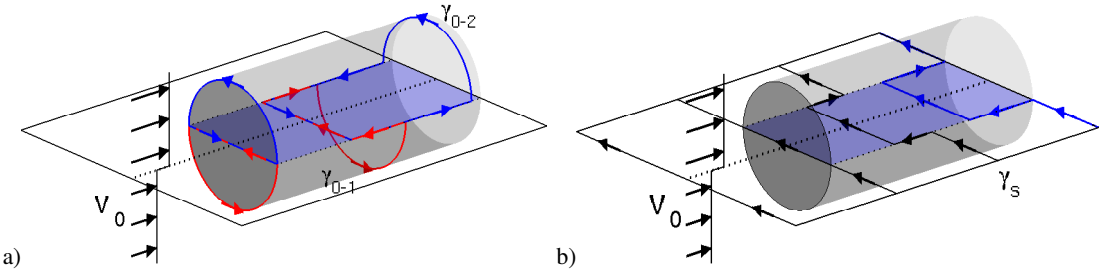

Figure 8. *3D sketch of non-uniformly loaded disc in a step shear with illustration of the deformation of wake and shear vorticity sheets; a) Deformation of wake vortex rings; b) Deformation of the vortex filaments which are responsible for the step shear.*

of the same non-uniformly loaded disc in a step shear as was considered in section 3.3. Figure 8a sketches the shape of the individual wake vortex rings at the position of the rotor and in the wake, respectively. As a consequence of the shear and/or the difference in loading between the two regions of the rotor, the outer part of the vortex rings moves with another velocity than the part at their intersection and therefore the vortex rings will be increasingly stretched with downstream position.

The stretching of the shear vorticity sheet is illustrated in 8b. Upstream of the rotor the entire span of the infinitely long shear layer vortex filaments are convected with the same velocity and therefore they remain straight here. Downstream of the rotor the vortex filaments will be deformed at the wake edges because of the difference in velocity inside and outside of the wake.

Due to the stretching of the wake and shear layer vorticity sheets, axial vorticity is formed at the intersection between the shear vorticity layer and the edges of the wake. However, from Figure 8 it is evident that axial vorticity is generated in opposing directions: the upper wake vortex rings are responsible for producing axial vorticity in the flow direction whereas the opposite is true for the lower wake vortex rings and the shear layer vorticity sheets. Nevertheless, if there is a net production of axial vorticity in one direction this will induce a velocity component perpendicular to the flow direction. This in turn would cause the shear layer and wake vorticity sheets to be deflected in the direction perpendicular to the flow direction and thus resulting in different velocities on the rotor than would have been the case if the axial vorticity production had been neglected. In the following we will therefore use our model to calculate the total axial vorticity produced by the interaction of the wake and the shear.

3.4.1 Axial vorticity from wake-shear interaction

The axial vorticity at a given streamwise position z can be determined by integrating the vorticity entering and exiting an infinitesimal cylinder enclosing the junction between the wake border and the shear sheet layer from 0 to z.

https://doi.org/10.5194/wes-2022-94
Preprint. Discussion started: 17 October 2022

eawe european academy of wind energy
Open Access WIND ENERGY SCIENCE DISCUSSIONS

The contribution from the wake stretching is then:

$$\Gamma_{z,\text{wake}} = \int_0^z (\gamma_{0-2} - \gamma_{0-1} + \gamma_{2-1})\, dz \tag{30}$$

where γ_{0-1}, γ_{0-2} and γ_{2-1} are the strength of the vorticity sheets released from the rotor and are determined from equations (21)-(23).

The corresponding contribution from the deformation of the shear layer vorticity sheet is

$$\Gamma_{z,\text{shear}}(z) = \int_0^z (\gamma_{s,w} - \gamma_s)\, dz = \int_0^z \Delta\gamma_s dz \tag{31}$$

where $\Delta\gamma_s$ is defined in equation (24).

From equations (26) and (27) we know that

$$\gamma_{2-1} + \Delta\gamma_s = \gamma_{0-1} - \gamma_{0-2} \tag{32}$$

From Equation (32) it is clear that Equations (30) and (31) exactly balances each other out and therefore there is no net production of axial vorticity which means that the present model predicts that there is no vertical movement of the wake and hence also no change in the power coefficient for a non-uniformly loaded rotor in sheared inflow. Note that the result of no net production of axial vorticity is general, which means that it also holds in the case without shear.

4 Discussion

In the following we will relate the results of our model to the findings of the aforementioned literature.

The conclusion that the power coefficient (defined in terms of the actual available power) of an idealized rotor is unaltered by the presence of a 1D shear is in agreement with the CFD simulation by Zahle and Sørensen (Zahle and Sørensen, 2010) as well as the work by Chammoro and Arndt (Chamorro and A Arndt, 2013). However, in contrast to the latter study we do not assume self-similarity between the velocity profiles far upstream and downstream in order to arrive at this result. Furthermore, our conclusion is based on a generic study, whereas the simulations by Zahle and Sørensen Zahle and Sørensen (2010) was carried out on a specific rotor and hence it is unknown to which extent their findings depends on the rotor and operational conditions used.

Since our model does not predict any formation of axial vorticity, it also does not predict a vertical deflection of the wake, which is in agreement with the studies by Branlard et al. (2015) and Ramos-García et al. (2018). In the CFD simulation by Zahle and Sørensen (Zahle and Sørensen, 2010), this effect is implicitly included and the downward velocity component that they observe upstream of the rotor is an indication that axial vorticity is in fact generated in the wake. This suggest that an ideal rotor might actually get a higher power coefficient in sheared inflow. The production of axial vorticity could be included in our model by assuming the transport velocity of the wake vorticity to change gradually from its value at the disc to that in the far wake. The absence of vertical motion of the wake as predicted by our method is in agreement with what would be found

https://doi.org/10.5194/wes-2022-94
Preprint. Discussion started: 17 October 2022

eawe european academy of wind energy
Open Access WIND ENERGY SCIENCE DISCUSSIONS

from a momentum analysis of the same situation: There are no vertical forces acting from the rotor on the flow[2] and therefore a control volume analysis of momentum conservation would show no vertical displacement of the wake.

5 Conclusions

We presented a simple analytical model based on inviscid vortex theory and applied it to model a rotor in uniform and non-uniform inflow.

Even though the model is based on a number of crude assumptions such as neglecting wake expansion and using a wake convection that is constant along each emission location, we showed that the model gives results that are identical to classical $1D$ momentum theory when applied to a uniformly loaded rotor operating in uniform inflow.

The application of the model to a non-uniformly loaded rotor operating in uniform inflow showed that any stream element through the rotor disc behaves locally as predicted by 1D momentum theory. As a consequence the model predicts that each stream element through the disc is both radially and tangentially independent from each other.

For a non-uniformly loaded rotor operating in non-uniform inflow our model predicts that the results from 1D momentum theory can be applied locally. Therefore, when the power coefficient is defined using the local free-stream velocity, we found that the power coefficient of an ideal rotor is unaltered by the presence of shear.

These findings indicate that the effects of shear and uneven loading in BEM-based codes should be treated in a local sense, and that concepts such as average disc/annulus loading and induction should be avoided.

Finally, by studying the inherent deformation of the wake vorticity sheet and the wind shear vorticity sheet, we concluded that there is no net generation of axial vorticity. The effects of the deformation of the rotor wake vorticity due to the shear and effects of the deformation of the shear vorticity due to the rotor exactly cancel each other out. This mean that there is no resulting cross-shear induced velocities and therefore also no cross-shear deflection of the wake.

The result that the production of axial vorticity due to the deformation of the wake and shear vorticity cancel each other out indicate that this effect has to be included in free wake vortex models. Omission of the effect of the deformation of the vorticity that create the shear will result in a non-physical upward motion of the wind turbine wake in free vortex models.

Author contributions. MG derived the model. NT wrote most of the manuscript and supported the analysis. EM contributed to the idea and derived the proofs in appendix. All three reviewed and edited the manuscript

Competing interests. The authors declare that they have no conflict of interest.

[2]Equation 2 show that for a finite thrust force, the tangential forces from the rotor on the flow tends to zero as the rotational speed tends to infinity.

https://doi.org/10.5194/wes-2022-94
Preprint. Discussion started: 17 October 2022

310 *Acknowledgements.* This work is funded by DTU Wind Energy

https://doi.org/10.5194/wes-2022-94
Preprint. Discussion started: 17 October 2022

eawe european academy of wind energy
Open Access WIND ENERGY SCIENCE DISCUSSIONS

References

Betz, A.: Das maximum der theoretisch möglichen ausnützung des windes durch windmotoren, Zeitschrift für das gesamte Turbinewessen, pp. 307–309, 1920.

Boorsma, K., Schepers, G., Aagard Madsen, H., Pirrung, G., Sørensen, N., Bangga, G., Imiela, M., Grinderslev, C., Meyer Forsting, A., Zhong Shen, W., Croce, A., Cacciola, S., Schaffarczyk, A. P., Lobo, B., Blondel, F., Gilbert, P., Boisard, R., Höning, L., Greco, L., Testa, C., Branlard, E., Jonkman, J., and Vijayakumar, G.: Progress in validation of rotor aerodynamic codes using field data, Wind Energy Science Discussions, 2022, 1–31, https://doi.org/10.5194/wes-2022-51, 2022.

Branlard, E.: Wind Turbine Aerodynamics and Vorticity-Based Methods, Springer, https://doi.org/10.1007/978-3-319-55164-7, 2017.

Branlard, E. and Gaunaa, M.: Cylindrical vortex wake model: right cylinder, Wind Energy, 18, 1973–1987, https://doi.org/https://doi.org/10.1002/we.1800, 2015.

Branlard, E. and Gaunaa, M.: Superposition of vortex cylinders for steady and unsteady simulation of rotors of finite tip-speed ratio, Wind Energy, 19, 1307–1323, 2016.

Branlard, E., Papadakis, G., Gaunaa, M., Winckelmans, G., and Larsen, T. J.: Aeroelastic large eddy simulations using vortex methods: unfrozen turbulent and sheared inflow, Journal of Physics: Conference Series, 625, 012 019, https://doi.org/10.1088/1742-6596/625/1/012019, 2015.

Chamorro, L. P. and A Arndt, R.: Non-uniform velocity distribution effect on the Betz–Joukowsky limit, Wind Energy, 16, 279–282, https://doi.org/https://doi.org/10.1002/we.549, 2013.

Glauert, H.: Airplane Propellers, vol. Aerodynamic Theory Volume IV, W. F. Durand, The Dover Edition (UK), 1963.

Grasso, F.: Ground and Wind Shear Effects in Aerodynamic Calculations, Tech. Rep. ECN-E–10-016, Energy research center of the Netherlands (ECN), 2010.

Johnson, W.: Rotorcraft Aeromechanics, Cambridge Aerospace Series, Cambridge University Press, https://doi.org/10.1017/CBO9781139235655, 2013.

Lanchester, F.: A contribution to the theory of propulsion and the screw propeller, Transaction of the Institute of Naval Architects, 56, 135–153, 1915.

Madsen, H., Mikkelsen, R., Johansen, J., Bak, J. amd Øye, S., and Sørensen, N.: Inboard rotor/blade aerodynamics and its influence on blade design. Chapter in Risø report Research in aeroelasticity EFP-2005 , Tech. Rep. Risø-R-1559(EN), Risø, National Laboratory, 2006.

Madsen, H. A., Riziotis, V., Zahle, F., Hansen, M., Snel, H., Grasso, F., Larsen, T., Politis, E., and Rasmussen, F.: Blade element momentum modeling of inflow with shear in comparison with advanced model results, Wind Energy, 15, 63–81, https://doi.org/https://doi.org/10.1002/we.493, 2012.

Magnusson, M.: Near-wake behaviour of wind turbines, Journal of Wind Engineering and Industrial Aerodynamics, 80, 147–167, https://doi.org/https://doi.org/10.1016/S0167-6105(98)00125-1, 1999.

Micallef, D., Ferreira, C., Sant, T., and van Bussel, G.: An Analytical Model of Wake Deflection Due to Shear Flow, 3rd Conference on The science of making Torque from Wind, Crete, Greece, pp. 337–347, 2010.

Øye, S.: A simple vortex model, Proc. of the third IEA Symposium on the Aerodynamics of Wind Turbines, ETSU, 70–73, 1990.

Ramos-García, N., Spietz, H. J., Sørensen, J. N., and Walther, J. H.: Vortex simulations of wind turbines operating in atmospheric conditions using a prescribed velocity-vorticity boundary layer model, Wind Energy, 21, 1216–1231, https://doi.org/https://doi.org/10.1002/we.2225, 2018.

https://doi.org/10.5194/wes-2022-94
Preprint. Discussion started: 17 October 2022

Sezer-Uzol, N. and Uzol, O.: Effect of steady and transient wind shear on the wake structure and performance of a horizontal axis wind turbine rotor, Wind Energy, 16, 1–17, https://doi.org/10.1002/we.514, 2013.

Shen, X., Zhu, X., and Du, Z.: Wind turbine aerodynamics and loads control in wind shear flow, Energy, 36, 1424–1434, https://doi.org/https://doi.org/10.1016/j.energy.2011.01.028, 2011.

Troldborg, N., Sørensen, J., Mikkelsen, R., and Sørensen, N.: A simple atmospheric boundary layer model applied to large eddy simulations of wind turbine wakes, Wind Energy, 17, 657–669, https://doi.org/10.1002/we.1608, 2014.

Zahle, F. and Sørensen, N.: Navier-Stokes Rotor Flow Simulations with Dynamic Inflow., Torque Conference, Crete, Greece, 2010.

Appendix A: Detailed derivation of Equation (8)

In order to derive Equation (8) we assume a constant convection velocity of the vorticity surface in the longitudinal direction, noted $\dot{z}$. During a time interval δt, the angle covered by a blade is $d\theta = \Omega dt$, and the downstream distance traveled by the vorticity is $dz = \dot{z}dt$. This leads to the following "helical" relationship between the coordinates:

$$\frac{d\theta}{dz} = \frac{\Omega}{\dot{z}} \qquad \frac{dz}{d\theta} = \frac{\dot{z}}{\Omega} \tag{A1}$$

We note that the quantity $h = 2\pi\dot{z}/\Omega$ is referred to as the "helical pitch" of the wake. From Figure 3, the trailed vorticity flux through a surface $dS = dzdr$ is $\gamma(z)dz$, which is equal to the elementary circulation passing though it, $d\Gamma_b(\theta)$:

$$d\Gamma_b(\theta) = \gamma(z)dz \tag{A2}$$

Integrating across a full rotor revolution, using Equation A1, and assuming that γ does not vary with z (a consequence of the assumption of constant convection velocity):

$$\Delta\Gamma = \int_0^{2\pi} d\Gamma_b(\theta) = \int_0^{2\pi} \gamma(z)dz = \gamma \int_0^{2\pi} dz = \gamma \int_0^{2\pi} \frac{\dot{z}}{\Omega} d\theta = 2\pi\gamma\frac{\dot{z}}{\Omega} \tag{A3}$$

or

$$\gamma = \frac{\Delta\Gamma\Omega}{2\pi\dot{z}} \tag{A4}$$

The same expression can be derived for the shed vorticity by following similar steps as used here for the trailed vorticity.

Appendix B: Induction of an infinitely long cylinder of tangential vorticity

Consider an infinitely long cylinder surface of tangential vorticity γ, which is aligned with the z-axis and has an arbitrary cross-section, see Figure B1. In the following we will show that this vortex cylinder induces a velocity in the z-direction of $W_z = \gamma$ on the inside and zero on the outside of the cylinder.

The proof is carried out in steps by proving the following 5 statements:

https://doi.org/10.5194/wes-2022-94
Preprint. Discussion started: 17 October 2022

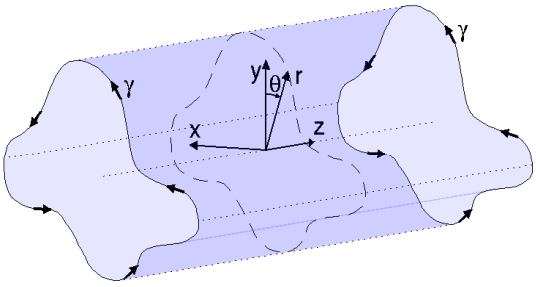

Figure B1. *Sketch of infinitely long cylinder of tangential vortex density γ with an arbitrary cross-section.*

1. The vortex cylinder only induces velocity in the z-direction, i.e. $W = W_z(r, \theta, z)$
2. The velocity is constant along z, i.e. $W_z = W_z(r, \theta)$
3. The velocity inside and outside of the cylinder is constant and equal to $W_z = W_{z,in}$ and $W_z = W_{z,out}$, respectively.
4. The outside velocity is $W_{z,out} = 0$
5. The velocity inside of the cylinder is $W_{z,in} = -\gamma$

To prove the first statement consider Figure B2 which shows a lateral cut of the cylinder. By virtue of the Biot-Savarts law the

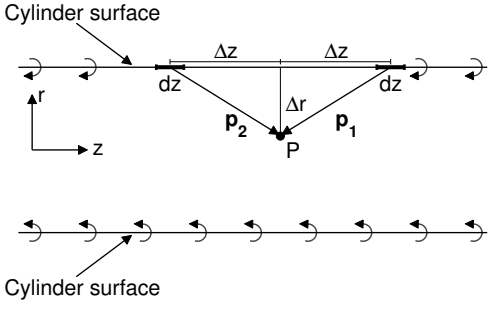

Figure B2. *A 2D cut of the vortex cylinder with definition of vectors* $\mathbf{p_1}$ *and* $\mathbf{p_2}$

velocity induced in a point P by a segment of the cylinder surface is:

$$d\mathbf{W}_i = \frac{\gamma dz}{4\pi} \frac{d\mathbf{s}_\theta \times \mathbf{p}_i}{|\mathbf{p}_i|^3} \tag{B1}$$

where $i = \{1, 2\}$, $\mathbf{p}_i$ is the vector from the segment to P and $\mathbf{s}_\theta$ is an infinitesimal vector in the azimuth direction.

Now consider two segments on the cylinder surface, which as shown in Figure B2 are located at the same azimuth position, θ but are located Δz and $-\Delta z$, respectively from P. Due to symmetry the radial velocities induced by these two segments

https://doi.org/10.5194/wes-2022-94
Preprint. Discussion started: 17 October 2022

eawe european academy of wind energy
Open Access WIND ENERGY SCIENCE DISCUSSIONS

cancel out. Since there for all segments on the cylinder surface is a corresponding segment which exactly cancels out the radially induced velocity in point P it follows that the total induction of the cylinder is in the z-direction, only. This can also be obtained by noting that each z-plan is a plan of symmetry for the vorticity distribution so that the velocity has to be orthogonal to these plans.

The second statement follows from the invariance of the problem in the z-direction which implies that there are no dependence with respect to the variable z and the derivatives in the z-direction are zero. This could have also been used to directly prove the first statement in the plane $z = 0$.

The third statement is proven by introducing a rectangular control surface as shown in Figure B3. The length of the rectangle

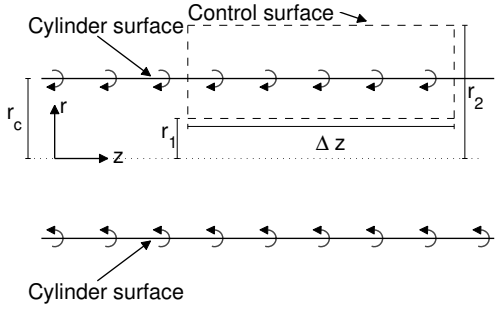

Figure B3. *A 2D cut of the vortex cylinder with definition of rectangular control surface*

is denoted Δz and its radial extent is from r_1 to r_2. Since the induction is only in the z-direction the circulation around the rectangle is:

$$\Gamma = (W_z(r_2,\theta) - W_z(r_1,\theta))\,\Delta z \tag{B2}$$

If the rectangle is not crossing the cylinder surface then the circulation around the rectangle is zero. Thus it follows that $W_z(r_2,\theta) = W_z(r_1,\theta) = W_{z,out}(\theta)$ for $r_2 > r_1 > r_c$ whereas $W_z(r_2,\theta) = W_z(r_1,\theta) = W_{z,in}(\theta)$ if $r_s > r_2 > r_1$.

The fourth statement follows by letting r_2 go towards infinity where the induction from the cylinder surface is 0, i.e. $W_{z,out} = 0$.

The fifth statement is proven by determining the circulation around the rectangular control surface when it is crossing the vortex cylinder and utilizing that $W_{z,out} = 0$, i.e

$$\Gamma = W_{z,in}\Delta z \Leftrightarrow W_{z,in} = -\gamma \tag{B3}$$

The induced velocity is thus independent of θ.